Winter Precipitation Microphysics Characterized by Polarimetric Radar and Video Disdrometer Observations in Central Oklahoma

GUIFU ZHANG AND SEAN LUCHS

School of Meteorology, and Atmospheric Radar Research Center, University of Oklahoma, Norman, Oklahoma

ALEXANDER RYZHKOV

Cooperative Institute for Mesoscale Meteorological Studies, Norman, Oklahoma

MING XUE

School of Meteorology, and Center for Analysis and Prediction of Storms, University of Oklahoma, Norman, Oklahoma

LILY RYZHKOVA

Northwestern University, Evanston, Illinois

QING CAO

Atmospheric Radar Research Center, and School of Electrical and Computer Engineering, University of Oklahoma, Norman, Oklahoma

(Manuscript received 14 July 2009, in final form 30 November 2010)

ABSTRACT

The study of precipitation in different phases is important to understanding the physical processes that occur in storms, as well as to improving their representation in numerical weather prediction models. A 2D video disdrometer was deployed about 30 km from a polarimetric weather radar in Norman, Oklahoma, (KOUN) to observe winter precipitation events during the 2006/07 winter season. These events contained periods of rain, snow, and mixed-phase precipitation. Five-minute particle size distributions were generated from the disdrometer data and fitted to a gamma distribution; polarimetric radar variables were also calculated for comparison with KOUN data. It is found that snow density adjustment improves the comparison substantially, indicating the importance of accounting for the density variability in representing model microphysics.

1. Introduction

Winter precipitation can have serious consequences, but the effects seen are dependent on the type of precipitation that reaches the surface. Winter storms such as freezing rain and heavy snow are responsible for billions of dollars of damage and can cause significant injury and death (Martner et al. 1992; Stewart 1992; Cortinas 2000; Cortinas et al. 2004). The processes that determine precipitation type can be very complex, resulting in liquid, frozen, and partially frozen precipitation (Zerr 1997). Even ''warm rain'' processes may result in freezing rain, increasing the complexity of winter precipitation scenarios (Rauber et al. 1994, 2000). An event can have freezing rain or ice pellets exclusively, periods of each, or the two may coexist (Stewart 1992); Rauber et al. (2001) presented a climatological description for such events in the United States. It is important to understand the microphysics of winter storms with different types of precipitation. In general, warm rain events are studied more thoroughly than winter events (Vivekanandan et al. 1999; Zhang et al. 2006; Henson et al. 2007). Although most studies using polarimetric radars focus on rain events,

Corresponding author address: Guifu Zhang, School of Meteorology, University of Oklahoma, 120 David L. Boren Blvd., Suite 5900, Norman, OK 73072.
E-mail: guzhang1@ou.edu

DOI: 10.1175/2011JAMC2343.1

some analyze winter events. Ibrahim et al. (1998) is one such work. Brandes et al. (2007) studied the microphysics of snow in Colorado using a 2D video disdrometer. Petersen et al. (2007) used a whole suite of ground-, air-, and space-based instruments to observe a snow event. Rasmussen et al. (2003), Tokay et al. (2007), and Bringi et al. (2008) looked into how variations in density affect the reflectivity factor of dry snow; this issue will be explored herein for other frozen and partially frozen particles in addition to dry snow. Although most winter precipitation studies focus on dry snow, Martner et al. (1993) included some mixed-phase precipitation but did not use polarimetric radar observations. Thurai et al. (2007) used polarimetric radar observations for winter precipitation not having the mixed phase.

There are also some studies that focus on various winter precipitation types. Trapp et al. (2001) used a polarimetric radar to observe a winter storm event with snow and mixed-phase precipitation in Oklahoma. Barthazy et al. (2001) used polarimetric radar data for detection and classification of hydrometeor types and then verified the data with ground-based in situ measurements. Yuter et al. (2006) used a disdrometer to investigate the physical properties of rain, mixed-phase precipitation, and wet snow. Raga et al. (1991) also focused on a winter storm with multiple types of precipitation using an instrumented plane to gather data. The instrumented aircraft is a valuable source of information—this method of gathering data is expensive, however, and is impractical to perform frequently over a long period of time or in weather that is potentially hazardous to the flight (Politovich 1996; Vivekanandan et al. 2001). In contrast, data collected with radar and disdrometers eliminate these shortcomings, and these instruments can obtain vast amounts of data on different precipitation types. For example, during the winter of 2006/07, data from both the National Severe Storms Laboratory (NSSL) polarimetric radar in Norman, Oklahoma, (KOUN) and the University of Oklahoma 2D video disdrometer (OU 2DVD) contain contributions from all-liquid, all-frozen, and mixed-phase precipitation. The dataset allows for a quantitative comparison study to characterize the precipitation physics.

This paper will present the observations of winter precipitation in central Oklahoma and the precipitation microphysics that are revealed. In section 2, the dataset collected by the NSSL KOUN and OU 2DVD is described. Methods used to calculate the polarimetric variables from the disdrometer data are presented in section 3. In section 4, polarimetric radar variables calculated from the disdrometer data are then compared with radar measurements to reveal the importance of the density variability for the observed winter events. A summary discussion and conclusions are provided in the last section.

2. Dataset

Data used for this study were collected using an S-band (11-cm wavelength) polarimetric weather radar (KOUN) and a 2D video disdrometer. The KOUN radar is a prototype dual-polarization Weather Surveillance Radar-1988 Doppler (WSR-88D) maintained and operated by NSSL. The radar measures reflectivity factor in horizontal polarization Z_H (or Z), differential reflectivity Z_{DR}, copolar cross-correlation coefficient ρ_{hv}, and differential phase ϕ_{DP} (Doviak and Zrnić 1993), and its data have been used extensively in hydrometeor classification and rain estimation (Zrnić and Ryzhkov 1999; Straka et al. 2000; Ryzhkov et al. 2005). The two measurements most important to this study are Z_H and Z_{DR}; these values for dry snow are usually lower than those for rain (Ryzhkov and Zrnić 1998).

The OU 2DVD was deployed on the University of Oklahoma's Kessler Farm Field Laboratory (KFFL). As seen in Fig. 1, KFFL is approximately 30 km from KOUN. At this distance, the disdrometer lies beyond the region of ground clutter but, with a beamwidth of about 500 m, is still close enough to the radar to ensure good resolution. In addition, the Washington site (WASH) of the Oklahoma Mesonet is also located at KFFL, providing surface observations of wind and temperature. As shown in Fig. 1, the OU 2DVD is a low-profile version (Schönhuber et al. 2008)—an updated version of that described by Kruger and Krajewski (2002). An example of its measurements, in the form of two images for each particle, is seen in Fig. 2.

The KOUN radar and the 2DVD data were collected during several precipitation events during the 2006/07 winter. These events had rain, snow, and mixed-phase precipitation, but most had periods of multiple types. The radar data were averages of volumes with 3×3 grid resolution measured at 0.5° above horizontal (i.e., 260 m above the KFFL ground level). The OU 2DVD data were available for all events, resulting in 7752 particle size distributions (PSDs) with 1-min resolution. To increase the number of particles for a PSD, particularly during periods of snow, these were condensed into 5-min PSDs, the same as that of Brandes et al. (2007).

There were four events over six days for which both radar and disdrometer data were collected: 30 November 2006, 12–14 January 2007, 27 January 2007, and 15 February 2007. The first three events contained transitions from liquid precipitation to frozen precipitation, and only snow fell during the 15 February event. The days most closely examined in this paper are 30 November 2006 and 27 January 2007. The precipitation associated with the 30 November event began with convection along a cold front and continued with stratiform precipitation. The early precipitation was primarily rain,

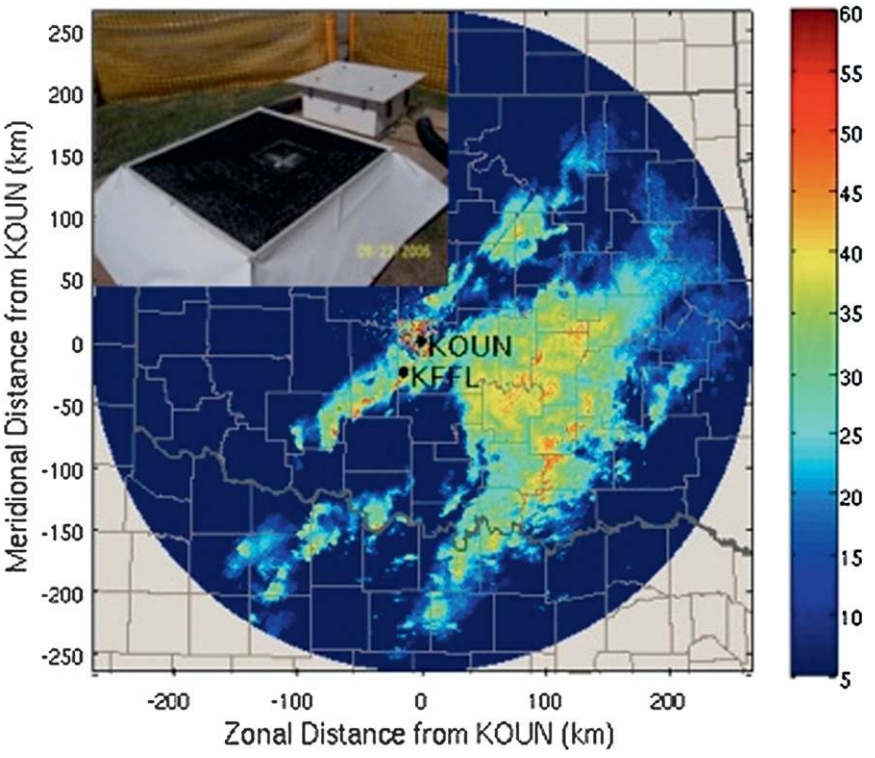

FIG. 1. A representative plan position indicator from KOUN showing the locations of the radar (KOUN) and Kessler Farm (KFFL), and also showing an inset image of the OU 2DVD.

which eventually made a transition into mixed-phase precipitation, which gave way to a period of snow (Scharfenberg et al. 2007). Typical particles measured by the 2DVD demonstrate this transition from raindrop (Fig. 2a) to ice pellet (Fig. 2b) and snowflakes (Figs. 2c,d). Figure 3 shows two rawinsonde-observation soundings and a Rapid Update Cycle (RUC) analysis sounding for Norman that correspond to the periods of different precipitation. The 0000 UTC 30 November soundings, during a time of freezing rain, show subfreezing temperatures at the surface under a strong inversion and warm layer. A considerably shallower warm nose exists at

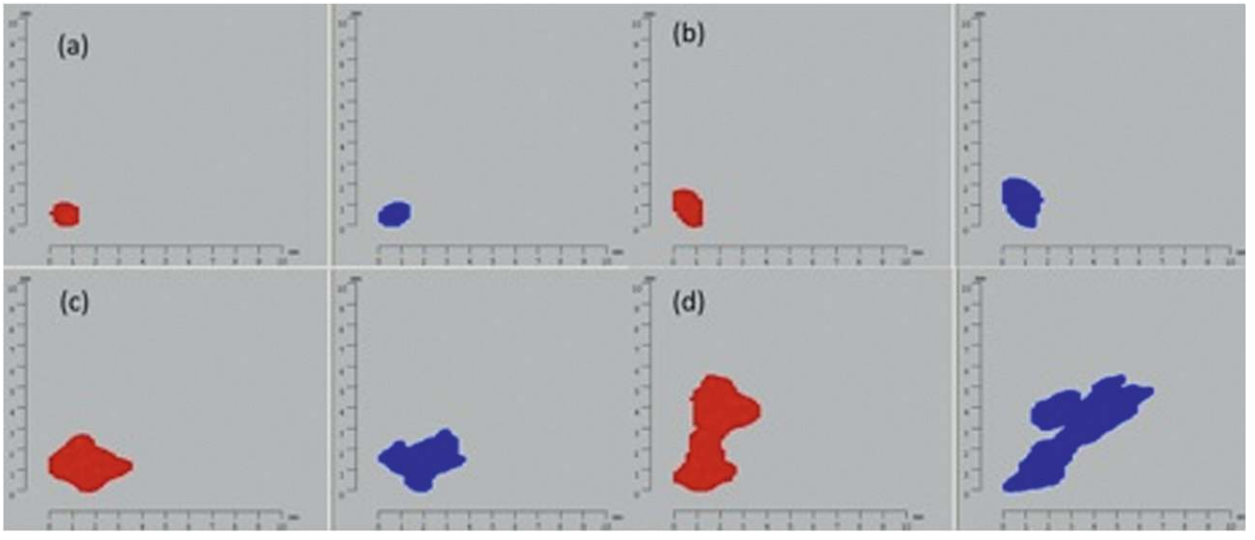

FIG. 2. Typical images of particles from the OU 2DVD. Front and side profiles of a particle are shown in red and blue, respectively: (a) a raindrop recorded at 0241 UTC, (b) an ice pellet from 1302 UTC, and (c),(d) snowflakes at 2218 UTC.

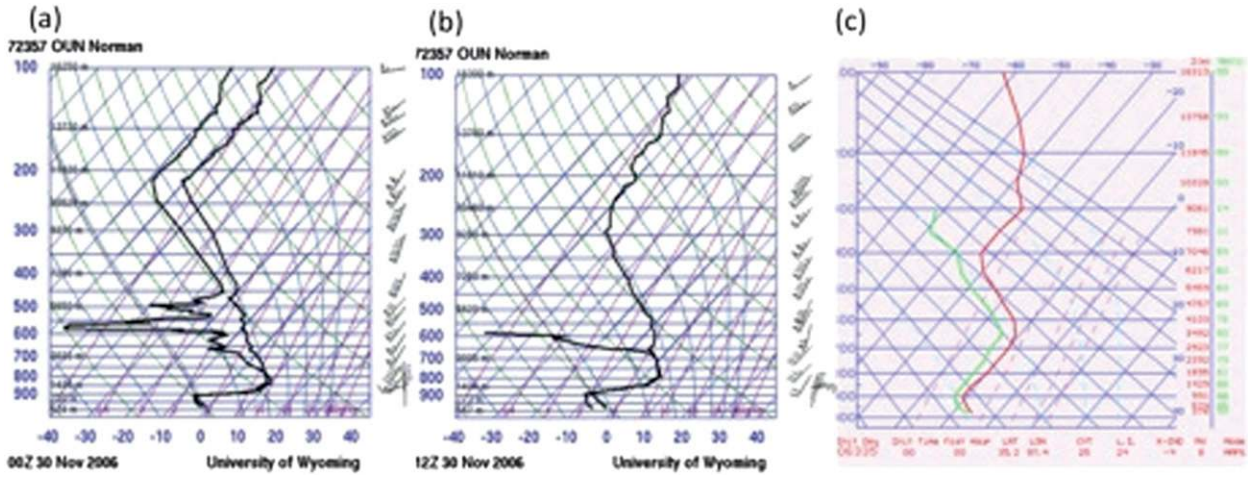

FIG. 3. Atmospheric soundings for Norman corresponding to the three precipitation types for the 30 Nov 2006 event from rawinsonde observations and RUC analysis at (a) 0000 UTC 30 Nov, (b) 1200 UTC on the same day, and (c) 0000 UTC 1 Dec (no radiosonde was launched at this time).

1200 UTC and corresponds to a transitional period of mixed-phase precipitation. The 0000 UTC RUC analysis for 1 December shows a column completely below freezing and corresponds to the period of snow later in the event. The precipitation on 27 January was also associated with the passage of a cold front. The initial precipitation fell as rain. Afterward, there was a break in precipitation, and then a second swath of precipitation fell as snow. The period of snow is interesting in that the surface temperature was still above freezing and saturation was reached, but this warm layer at the surface was not sufficiently warm or deep enough to melt the snow completely. Mesonet data show that the surface temperature at the Washington station is lower than earlier—very near freezing, showing little opportunity for melting. More analysis over the precipitation periods is presented in section 4.

3. Method

a. Calculation of radar variables

Using the data collected by the disdrometer, it is possible to model polarimetric radar variables for comparison with radar data. For horizontally and vertically polarized waves, the radar reflectivity factor can be calculated as (Zhang et al. 2001)

$$Z_{h,v} = \frac{4\lambda^4}{\pi^4 |K_w|^2} \int |f_{h,v}(D)|^2 N(D)\, dD, \qquad (1)$$

where λ is the radar wavelength; $K_w = (\varepsilon_w - 1)/(\varepsilon_w + 2)$, with ε_w being the relative dielectric constant of water; $f_{h,v}$, are the backscattering amplitudes of hydrometeors for horizontally and vertically polarized waves, respectively; and $N(D)$ is the PSD. For rain, the scattering amplitudes are found using the T-matrix scattering method. For snow, assuming that the particles are oblate spheroids within a Rayleigh regime, the scattering amplitudes can be determined using the following equation (Ishimaru 1991):

$$f_{h,v} = \frac{\pi^2 D^3}{6\lambda^2} \frac{\varepsilon - 1}{1 + L_{h,v}(\varepsilon - 1)}. \qquad (2)$$

Here, D is the equivolume sphere diameter, $L_{h,v}$ is a shape parameter, and ε is the relative dielectric constant of the particle. Further, $L_{h,v}$ are defined as

$$L_v = \frac{c^2}{1 + c^2}\left(1 - \frac{\arctan c}{c}\right), \quad \text{where} \quad c = [(a/b)^2 - 1]^{1/2}, \quad \text{and} \qquad (3)$$

$$L_h = \frac{1 - L_v}{2}, \qquad (4)$$

where a is the semimajor axis of the particle and b is the semiminor axis. The axis ratio b/a is fixed at 0.7 for frozen particles. The PSD measured by the disdrometer is also separated into PSDs that are treated as rain and as snow, in a manner similar to that of Yuter et al. (2006). The dielectric constant ε of the hydrometeor depends on the particle's composition. If it is water, then $\varepsilon = \varepsilon_w$, the dielectric constant of water. If the particle is dry snow, the following Maxwell-Garnett mixing formula is used (Ishimaru 1991):

$$\varepsilon = \varepsilon_s = \frac{1 + 2f_v y}{1 - f_v y}. \qquad (5)$$

Here, ε_s is the dielectric constant of dry snow, f_v is a fractional volume: ρ_s/ρ_i (where ρ_s is the density of snow and ρ_i is the density of solid ice). Also, $y = (\varepsilon_i - 1)/(\varepsilon_i + 2)$, where ε_i is the dielectric constant of ice. The dielectric constants are calculated at 0°C for the 11-cm wavelength, yielding $\varepsilon_w = (80.7, 23.9)$ and $\varepsilon_i = (3.17, 0.0039)$. The density of snow, as proposed by Brandes et al. (2007), is

$$\rho_s = 0.178D^{-0.922}, \tag{6}$$

where the diameter D is in millimeters and ρ_s is in grams per centimeter cubed. Equation (6) is very similar to the $\rho_s = 0.17D^{-1}$ found earlier by Holroyd (1971).

From these reflectivity factors expressed by (1), we can compute the 2DVD-derived $Z = 10\log_{10}(Z_h)$ in reflectivity decibels and differential reflectivity $Z_{\rm DR} = 10\log_{10}(Z_h/Z_v)$. These modeled data can be compared with the Z and $Z_{\rm DR}$ measurements from KOUN, averaged over nine resolution volumes arranged in a 3×3 grid above KFFL.

b. Density adjustment

It is noted that (6) is a statistical relation derived from disdrometer and gauge measurements of Colorado winter storms. While looking at the disdrometer data collected in Oklahoma, it became apparent that the density relation in (6) may not best describe the density of the snowfall during these events. Several factors could affect the density of frozen precipitation that cannot be described by one simple size–density relation. There are both in-cloud processes that affect the formation and growth of snowflakes and subcloud processes that affect the flake during its descent to the ground (Roebber et al. 2003). Figure 4 shows a plot of measured fall velocities on 30 November 2006. Also plotted is the empirically derived fall speed of raindrops (Brandes et al. 2002), and the lower curve is the empirically derived terminal velocity for snow particles (Brandes et al. 2007).

The curve plotted in the middle is used to separate the liquid and ice phases. Of primary interest are the plotted asterisks that signify particles in the snow portion of the event; most of the snow velocities measured in Oklahoma are larger than the predicted fall velocity using the Brandes density relation determined from the Colorado data. Hence, the density of these particles should be greater than that predicted by the fixed relation in (6).

Ways to improve the calculation of the dielectric constant were considered. Given that water is present in mixed-phase and wet snow particles, a Maxwell-Garnet mixture of water and snow could be used to create a more realistic dielectric constant. This approach requires knowledge of the amount of water present in a particle, however, which could not be directly measured by the radar or disdrometer. Thus, any mixture would have to be arbitrarily defined. To create a more realistic value of density, a terminal velocity–based modification to the density value was derived from the equation for terminal fall velocity [Pruppacher and Klett 1997, Eq. (10-138)]. The value for ρ_s from (6) is recast as a baseline density ρ_b, the measured velocity is represented by v_m, and we use a baseline velocity $v_{\rm bs}$ to create an estimate of ρ_s to replace (6):

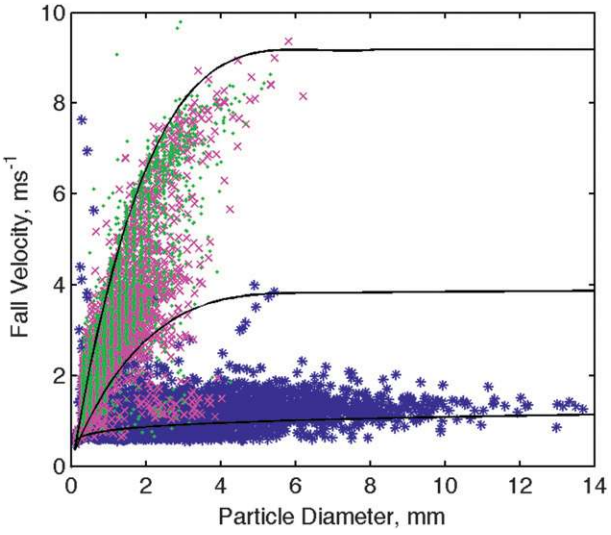

FIG. 4. Plot of fall velocity (m s^{-1}) vs diameter (mm) on 30 Nov 2006. Data from the freezing-rain period (0000–0800 UTC) are denoted by circles (green), data from the mixed-phase period (0800–1600 UTC) are denoted by times signs (purple), and data from the frozen-precipitation period (1600–0000 UTC) are denoted with an asterisk (blue). Also plotted are a fourth-degree polynomial approximation of raindrop terminal fall speed, a power-law relation for the terminal fall speed of snow, and the velocity function used to separate the rain and snow PSDs.

$$\rho_s = \alpha\rho_b, \tag{7a}$$

where

$$\alpha = \left(\frac{v_m}{v_{\rm bs}}\right)^2 \frac{\rho_{aO}}{\rho_{aC}}. \tag{7b}$$

Here, α is the adjustment, similar to the variable $f_{\rm rim}$ used in Ryzhkov et al. (2008). The terminology is changed slightly for generality. Although riming is frequently a significant factor in the variability of density for frozen precipitation, this adjustment is being used to estimate density variability for all factors rather than for one alone. Air densities (ρ_{aC} and ρ_{aO}) are estimated from the pressures at 1742 m MSL for Marshall Station, Colorado, and 344 m MSL for the Washington mesonet site on the KFFL in Oklahoma, respectively.

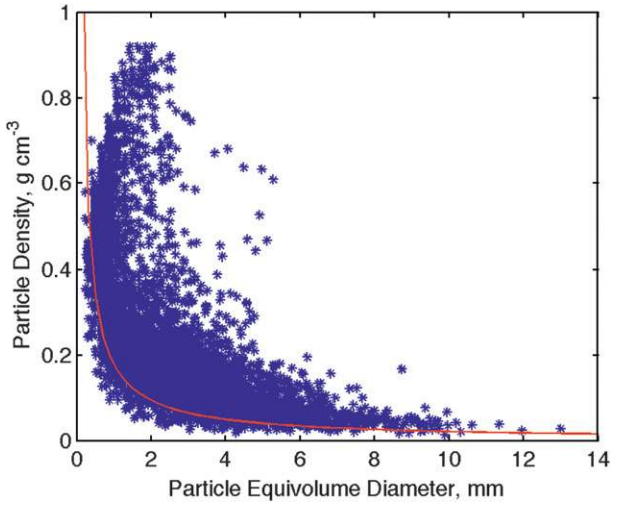

FIG. 5. Velocity-adjusted density vs diameter for 30 Nov 2006. Also plotted is the baseline density, from Brandes et al. (2007).

Because the particles in the snow PSD are treated as frozen, the density is capped at 0.92 g cm^{-3}. Figure 5 shows the adjusted densities as a function of particle size for the 30 November event. Results for these events were recalculated using (6) and (7) to determine how the calculated polarimetric radar variables were affected by this density adjustment.

4. Case studies

Using the 2DVD data, it was possible to compare reflectivity and differential reflectivity with those measured by KOUN and to study precipitation microphysics properties. Polarimetric variables were calculated from the disdrometer data using both the fixed density relationship, and the velocity-adjusted density relationship to see the impact of density variability.

a. 30 November 2006 event

Figure 6 shows the radar variables and the physical conditions for the event. As noted earlier, this event began with rain, mostly stratiform but with some convective cells, which continued through about 0800 UTC. A raindrop recorded at 0241 UTC is shown in Fig. 2a. A transitional period with mixed-phase precipitation becoming ice pellets then continued through about 1600 UTC, as confirmed by the 2DVD measurement of an ice pellet at 1302 UTC as shown in Fig. 2b. The rest of the day had primarily snow, as indicated by Figs. 2c and 2d for two snowflakes measured at 2218 UTC. The measured rain DSDs and snow PSDs are shown in Fig. 6c. Winds measured at the Washington mesonet site were in the vicinity of 7 m s^{-1} all day (Fig. 6d), and surface temperature changed from about −2°C for the rain period to below −5°C for the late period of snow (Fig. 6e), consistent with the phase change for the precipitating particles observed by the 2DVD.

Figures 6a and 6b show the comparison of reflectivity factor and differential reflectivity measured by KOUN and deduced from 2DVD measurements. The radar measurements are shown in solid blue, the calculations for the fixed snow density [(6)] are shown in red, and those for the density-adjusted snow [(7)] are shown in green. Early in the period, through about 0400 UTC, there is a generally good comparison between Z (dBZ) and Z_{DR} (dB) measured by KOUN and calculated from 2DVD data, even without the density adjustment. Just after 0400 UTC, there is a strange disconnect between the disdrometer and radar measurements. Given the otherwise good agreement between the two throughout the rain period except for this short stretch, there may have been an issue with the radar measurements. Also possible is that the rain measured by the disdrometer was part of a localized maximum in rain and was partially or completely lost in the averaging of the KOUN resolution volumes. After this short disconnect, the comparisons for both Z and Z_{DR} are again very good through the rest of the rain period—considering the seven orders of difference in the resolution volumes.

As the event makes a transition from rain to the mixed phase, we begin to see differences between the KOUN measurements and 2DVD calculations. Without the density adjustment, there can be significant differences—up to 15 dB for reflectivity. The underestimations by 2DVD data appeared to grow larger as the proportion of frozen precipitation increased. This is not a surprise because any portion of the PSD classified as frozen was treated as dry snow in this scheme, though the portion may have contained some fraction of liquid water or ice pellets, which would have larger dielectric constants and stronger radar returns than the modeled dry snowflakes for the same size of particles. There are also differences between KOUN and the disdrometer for Z_{DR}. When Z is underestimated by the disdrometer, so is Z_{DR}. When there is a higher concentration of frozen particles, calculated Z and Z_{DR} are both biased toward values that are too low.

Excluding the rain period (0000–1100 UTC), the mean Z and Z_{DR} biases are calculated as −12.04 and −0.22 dB, for the transition and snow periods (1100–0000 UTC), respectively, which values are possibly due to the underestimation of particle density with the fixed relation in (6). Using the velocity-adjusted density [(7)], the reflectivity and differential reflectivity are recalculated and are shown in green in Figs. 6a and 6b. For the snow period, the biases for Z and Z_{DR} are reduced significantly, to −4.85 and −0.062 dB, respectively—less than a one-half of those without density adjustment. The comparisons of Z and Z_{DR} are also shown in 1:1 scatterplots in Fig. 7. The

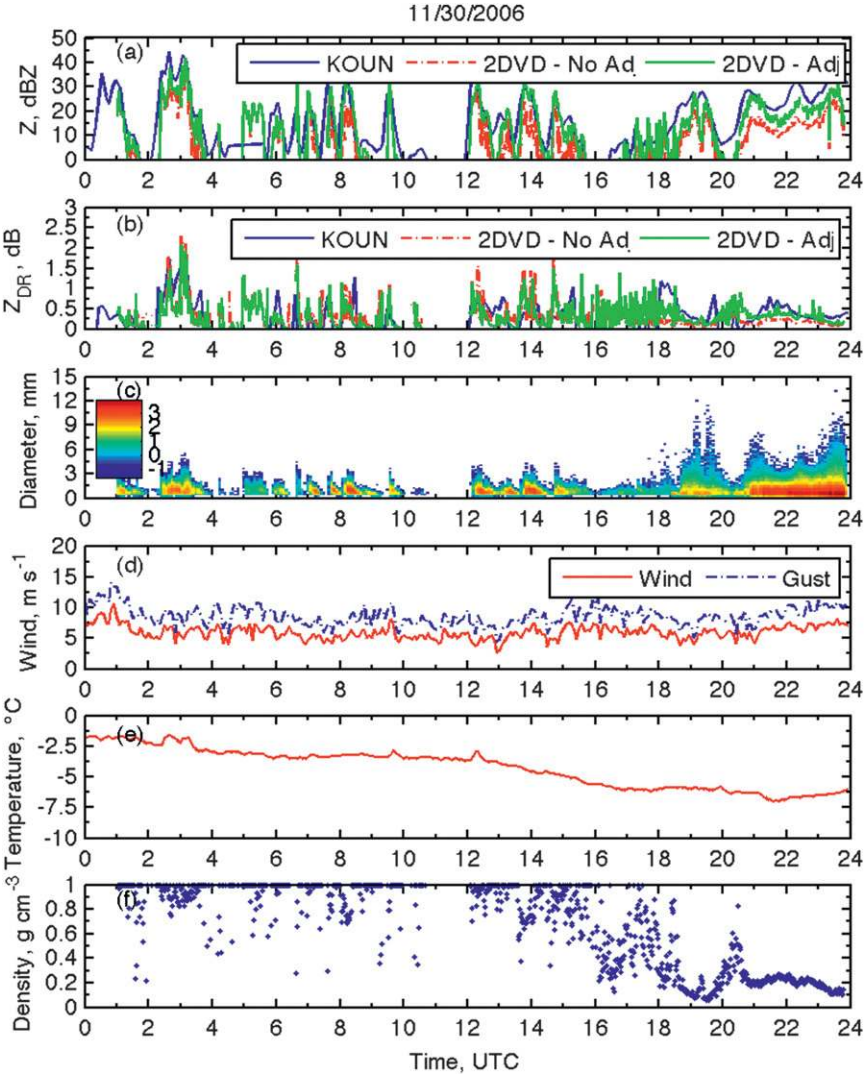

FIG. 6. Comparison of (a) Z and (b) Z_{DR} between KOUN measurements and 2DVD calculations with and without density adjustment for the 30 Nov 2006 event. (c) Measured DSDs and PSDs, (d) wind speed and gusts measured at WASH, (e) surface temperature measurements at WASH, and (f) derived volume-weighted density.

upper row of plots are those without density adjustment, and the lower row of plots are with density adjustment. The correlation coefficients are not improved much, but the data points align with the 1:1 line much better.

Throughout the entire event, many of the differences between the disdrometer calculations and the KOUN measurements have been eliminated with the density adjustment. The early rain period before 0400 UTC is very good, save for the time of the largest differences, which have still been improved some. The disconnect seen after 0400 UTC is still present and is largely unchanged, suggesting that there was indeed an issue with the KOUN data. Thereafter, the comparisons were very good through the rest of the rain period, however. KOUN and disdrometer Z_{DR} were close during the rain period, before and after using the velocity-adjusted density.

The improvements made in the disdrometer calculations may have been modest during the rain period, but it is during the mixed-phase and snow periods that they become more significant. The reflectivities for the disdrometer and KOUN are usually very close. Although there are still a few high peaks in Z_{DR} from the disdrometer, it matches with KOUN much better than using the fixed density relation. The early transition to snow is still somewhat rough—Z and Z_{DR} calculated from the disdrometer data are both noisy and sometimes contain more variations than in the previous scheme. Whereas the previous calculations were all lower than the KOUN

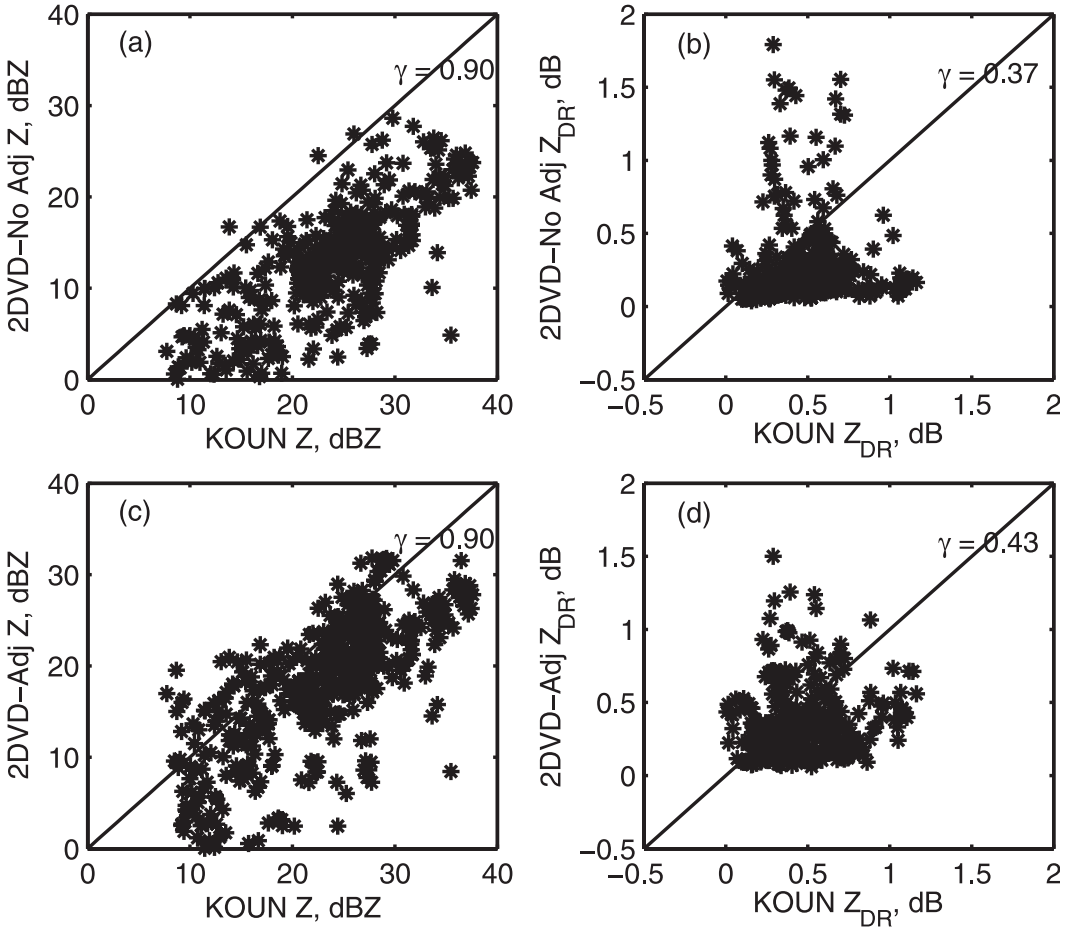

FIG. 7. Scatterplots of 2DVD-calculated Z and Z_{DR} with and without density adjustment vs KOUN measurements for the 30 Nov 2006 event: (a) Z without density adjustment, (b) Z_{DR} without density adjustment, (c) Z with density adjustment, and (d) Z_{DR} with density adjustment.

measurements, however, the new calculations tend to be closer to the KOUN measurements. As indicated by the reduction in the calculated biases, the most dramatic improvement came at the end of the event for the snow period. Much of the extreme difference in the reflectivity comparison has been eliminated, although some difference continues to exist. The Z_{DR} calculations and radar measurements are now very close.

The change from using the fixed density relation to one that is velocity adjusted highlights the importance of the variability of hydrometeor density to their scattering properties. Rasmussen et al. (2003), Tokay et al. (2007), and Bringi et al. (2008) noted a similar effect on reflectivity in dry snow data. The results from this study appear to confirm their findings and show that density variability is important in modeling not only reflectivity but also differential reflectivity. Wet snow and mixed-phase precipitation, in addition to dry snow, experience effects from density variability. Comparisons of the volume-weighted density (Fig. 6f) with the temperature (Fig. 6d) measured at the Washington mesonet site also provide a connection with recent work by Brandes et al. (2008) and Jung and Zawadzki (2008). Both found that the terminal fall velocity of snow increased with temperature, implying a higher density.

Although the radar–disdrometer comparison is improved significantly with the density adjustment, some differences still remain. A number of sources could explain the differences. These include sampling-volume difference, wind effects, and measurement errors. The KOUN resolution volume over the disdrometer is approximately 5×10^7 m^3 and is much larger than the sampling volume of the 2DVD (about 5 m^3). The precipitation measured by KOUN and that measured by the disdrometer could be different. Although wind advection effects studied by Barthazy et al. (2001) and Rasmussen et al. (2003) could be small for this dataset because the radar beam center is only 260 m above the disdrometer, wind effects on the 2DVD measurements could be significant as a result of altering the airflow and causing undercatching (Nešpor

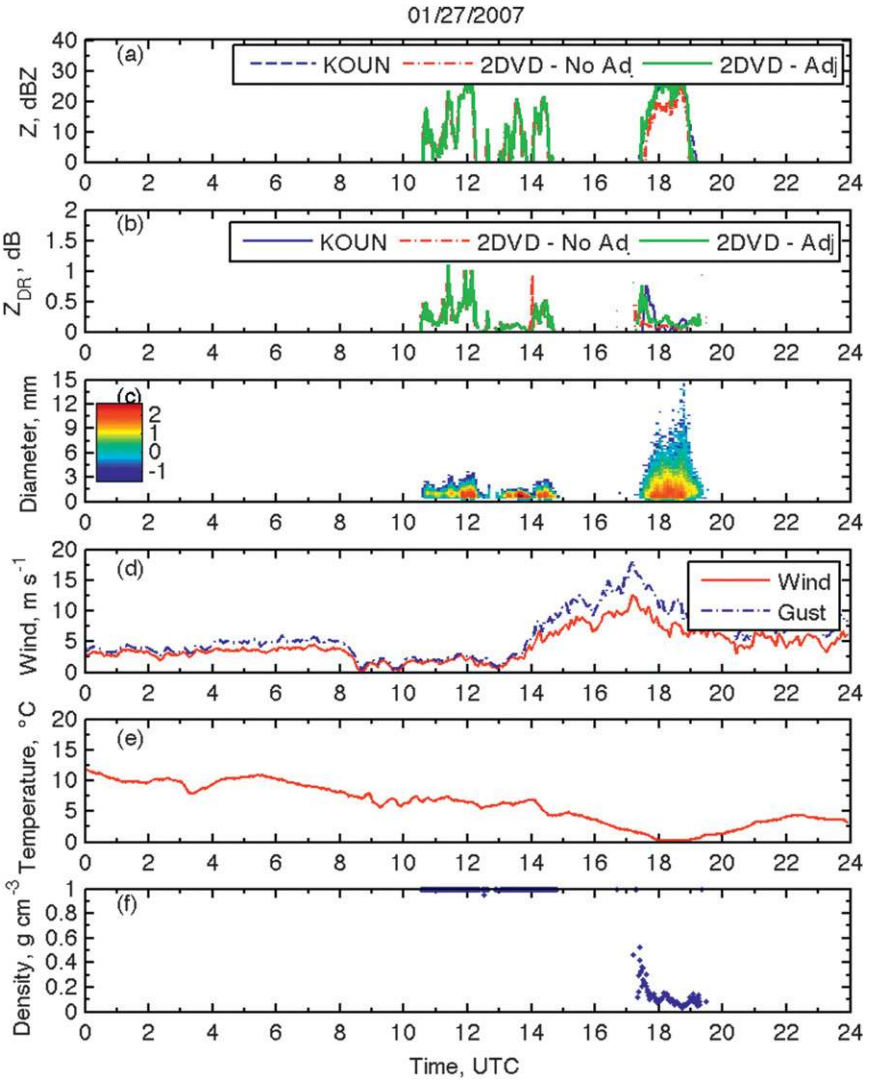

FIG. 8. As in Fig. 6, but for 27 Jan 2007.

et al. (2000). Another issue may arise from uncertainty in the measurements. Drop mismatching and multiple drops positioned such that they appear as one particle to the disdrometer could result in errors (Thurai and Bringi 2005). Radar measurements themselves have errors: ~1–2 dB for Z and ~0.2 dB for Z_{DR}. Doubling these numbers would be possible for the comparison. Because of these factors, it may be unrealistic to expect a perfect match between the radar measurements and disdrometer calculations.

b. 27 January 2007 event

Figure 8 shows the results for the 27 January event. This event was unique in that it had no mixed-phase precipitation. There was one period of rain, followed by a break in precipitation and then a period of snow. In contrast to the other event, the warmest air on this day was in a shallow layer near the surface. As a result, when snow fell, it began as wet snow and then gradually became dry snow as the warm layer cooled and the surface temperature approached 0°C. The Z and Z_{DR} comparisons appear to confirm this scenario. Without density adjustment, the comparison between KOUN and the disdrometer worsens as the snow begins at 1730 UTC, with the disdrometer calculations of Z and Z_{DR} being lower than the corresponding KOUN measurements. As the snow becomes more like dry snow beginning at 1830 UTC, Z and Z_{DR} match more closely.

When the adjusted density relation in (7) is used, the overall agreement between Z and Z_{DR} calculations and the radar measurements is good. As shown in Table 1, the mean Z and Z_{DR} biases reduce to (0.60, 0.034) from

TABLE 1. Comparison of radar variables between disdrometer and radar measurements.

Variables	1100 UTC 30 Nov–0000 UTC 1 Dec 2006		1600 UTC 27 Jan–0000 UTC 28 Jan 2007		0000–8000 UTC 15 Feb 2007	
	No density adjustment	With density adjustment	No density adjustment	With density adjustment	No density adjustment	With density adjustment
$\langle Z^{(D)} \rangle$ (dBZ)	10.47	17.26	16.53	22.30	0.14	2.47
$\langle Z_{\mathrm{DR}}^{(D)} \rangle$ (dB)	0.653	0.741	0.483	0.574	0.624	0.672
$\langle Z^{(D)} - Z^{(R)} \rangle$ (dB)	−11.64	−4.85	−6.37	−0.60	−8.01	−5.68
$\langle Z_{\mathrm{DR}}^{(D)} - Z_{\mathrm{DR}}^{(R)} \rangle$ (dB)	−0.149	−0.062	−0.057	0.034	−0.066	0.018

(−6.37, −0.057) for the situation without the density adjustment. The correlations between the disdrometer results and radar measurements are shown in Fig. 9 and indicate an improved comparison. Although the improvement does not appear in the correlation coefficients, this result may not be representative because there are only 54 data points for the statistical calculation.

Even with the improvement, there is still a difference between the two reflectivities in the middle of the snowfall. It seems to correspond to the lowest Z_{DR} and the lowest surface temperatures. The volume-weighted density appears to approach its minimum here. In looking at the PSD shown in Fig. 8c, the particle concentration across the range of diameters is seen to be lower here than at both the beginning and end of the snowfall. There are no large snowflakes, and there are definitely fewer medium-sized snowflakes. Even the number of smaller particles appears to be slightly lower than the surrounding PSDs. This difference also apparently corresponds to a short but noticeable increase in sustained winds and wind

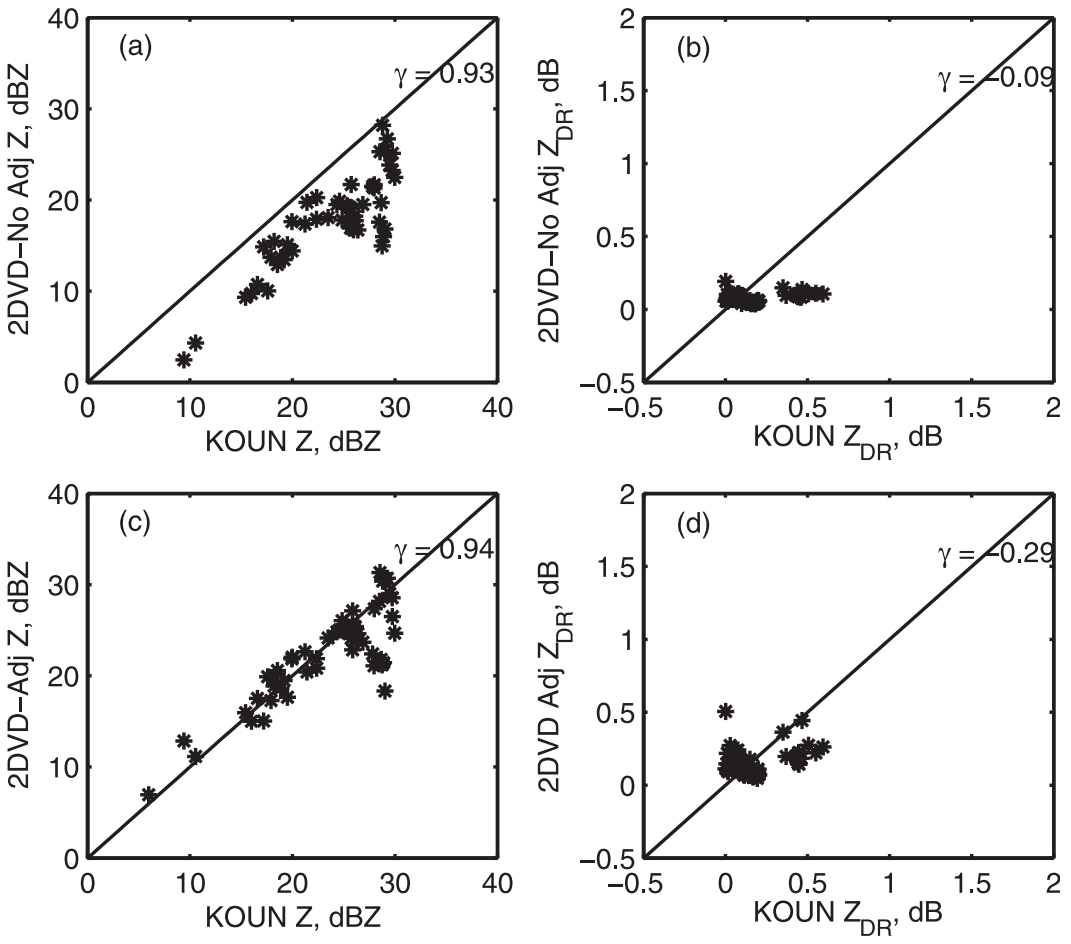

FIG. 9. As in Fig. 7, but for 27 Jan 2007.

gusts. It is possible that these winds blew away the largest particles and therefore they were simply not recorded. There were stronger winds as the snow began, but the density of these wet particles was considerably higher and would not be affected as much by the winds.

c. Other events from the 2006/07 winter

There were two other events during the 2006/07 winter that were observed by both the OU 2DVD and KOUN but are not discussed in depth in this paper. The period of 12–14 January 2007 was another event that featured a transition from rain in the wake of a passing cold front. Unlike other events, however, the rain shifted only to a period of mixed-phase precipitation at Kessler Farm. Scharfenberg et al. (2007) noted that there was a short period of light snow near KOUN, but this was not observed at Kessler Farm. As a result, many of the distributions measured by the OU 2DVD were very similar to rain in character, and the contributions of frozen scatterers were small. Because of this, there were only modest alterations to the calculation of Z and Z_{DR}, which are already similar to the values measured by KOUN.

The 15 January event, unlike the other winter precipitation events, was composed entirely of dry snow. This led to a similar situation as in the 12–14 January event. In this case, however, the frozen precipitation is generally described very well by the Brandes relation, and so incorporation of the density adjustment helps little. The mean biases for Z and Z_{DR} are (−8.01, 0.066) without density adjustment and (−5.68, 0018) with density adjustment. Early in the period, there are small variations in density that result in some modest improvement in the calculations of polarimetric variables, particularly during the heaviest snow. The snow was frequently so light during this event, however, that concerns about the data quality from KOUN arose for later portions of the event when reflectivity was less than 0 dBZ, limiting the improvement of the comparison.

5. Conclusions and discussion

Observations of several winter precipitation events were made during 2006/07 by the polarimetric KOUN radar and a 2D video disdrometer deployed at the Kessler Farm Field Laboratory. The disdrometer data were used to calculate radar variables Z and Z_{DR}, which were then compared with KOUN data. Without density adjustment, the initial comparisons between the two datasets for the events showed that, although the general patterns matched throughout an event, there is not good agreement. It was also found that the scattering amplitudes of frozen precipitation could be calculated more accurately using a variable density adjustment factor, which is determined from the fall velocities measured by the disdrometer. After recalculation of the radar variables from disdrometer data, much better agreement was found with KOUN data in most cases. The improvements were greatest when precipitation was not dominated by rain or dry snow, making it clear that variability in density has a very important role in modeling the scattering properties of winter hydrometeors of all types. The improved agreement for Z and Z_{DR} between the OU 2DVD and KOUN shows that it is possible to attempt a microphysics retrieval from the KOUN data not just for rain but for other winter hydrometeors as well.

It is not surprising to see the variation of the comparisons because snow particle density for each storm can differ from the mean relation used for calculations. Exact agreements between the radar and disdrometer should not be expected because of differences in resolution volumes, wind effects, and measurement errors, as well as the change in particle density from storm to storm and from time to time. Further improvements may be made to the calculations for graupel, however. Following Yuter et al. (2006) and creating a graupel category, as well as adjusting the density from a new baseline graupel density, could result in improved density estimation for that type of precipitation. It may also help to adjust near-rain precipitation that should have their scattering amplitudes modified but currently do not. Also, reintroducing a water–ice mixture for partially frozen precipitation could make both the rain and snow PSD categories more realistic. It would be necessary to find a way to deduce the amount of water present from the disdrometer data to accomplish this task, however. Adopting a variable function for the axis ratio would help the axis ratio situation while keeping the relative computational efficiency of using binned disdrometer data.

Acknowledgments. This work was supported by NSF Grant ATM-0608168. The authors thank Drs. Edward Brandes and Richard J. Doviak for helpful discussions, Dr. Terry Schuur and others at NSSL for collecting the KOUN data, and Ms. Hyang-Suk Park for her help in working with the KOUN data. We also thank the anonymous reviewers for their comments and suggestions. The mesonet data were collected by the Oklahoma Climate Survey (OCS). Atmospheric sounding data were provided by the University of Wyoming (online at http://weather.uwyo.edu/upperair/sounding.html). RUC analysis data were obtained from the NASA Langley Cloud and Radiation Research group (online at http://www-angler.larc.nasa.gov/cgi-bin/satimage/sounding.cgi).

REFERENCES

Barthazy, E., S. Goke, J. Vivekanandan, and S. M. Ellis, 2001: Detection of snow and ice crystals using polarization radar

measurements: Comparison between ground-based in-situ and S-Pol observation. *Atmos. Res.,* **59–60,** 137–162.

Brandes, E. A., G. Zhang, and J. Vivekanandan, 2002: Experiments in rainfall estimation with a polarimetric radar in a subtropical environment. *J. Appl. Meteor.,* **41,** 674–685.

——, K. Ikeda, G. Zhang, M. Schonhuber, and R. M. Rasmussen, 2007: A statistical and physical description of hydrometeor distributions in Colorado snowstorms using a video disdrometer. *J. Appl. Meteor. Climatol.,* **46,** 634–650.

——, ——, and G. Thompson, 2008: Aggregate terminal velocity/temperature relations. *J. Appl. Meteor. Climatol.,* **47,** 2729–2736.

Bringi, V. N., G.-J. Huang, D. Hudak, R. Cifelli, and S. A. Rutledge, 2008: A methodology to derive radar reflectivity-liquid equivalent snow rate relations using C-band radar and a 2D video disdrometer. *Proc. Fifth European Conf. on Radar in Meteorology and Hydrology,* Helsinki, Finland, EUMETSAT, 5 pp. [Available online at http://erad2008.fmi.fi/proceedings/extended/erad2008-0070-extended.pdf.]

Cortinas, J., Jr., 2000: A climatology of freezing rain in the Great Lakes region of North America. *Mon. Wea. Rev.,* **128,** 3574–3588.

——, B. C. Bernstein, C. C. Robbins, and J. W. Strapp, 2004: An analysis of freezing rain, freezing drizzle, and ice pellets across the United States and Canada: 1976–90. *Wea. Forecasting,* **19,** 377–390.

Doviak, R. J., and D. S. Zrnić, 1993: *Doppler Radar and Weather Observations*. 2nd ed. Academic Press, 562 pp.

Henson, W., R. Stewart, and B. Kochtubajda, 2007: On the precipitation and related features of the 1998 ice storm in the Montréal area. *Atmos. Res.,* **83,** 36–54.

Holroyd, E. W., III, 1971: The meso- and microscale structure of Great Lakes snowstorm bands—A synthesis of ground measurements, radar data, and satellite observations. Ph.D. dissertation, State University of New York at Albany, 148 pp.

Ibrahim, I. A., V. Chandrasekar, V. N. Bringi, P. C. Kennedy, M. Schoenhuber, H. E. Urban, and W. L. Randen, 1998: Simultaneous multiparameter radar and 2D-video disdrometer observations of snow. *Proc. Geoscience and Remote Sensing Symp. (IGARSS '98),* Vol. 1, Seattle, WA, IEEE, 437–439.

Ishimaru, A., 1991: *Electromagnetic Wave Propagation, Radiation, and Scattering*. Prentice Hall, 637 pp.

Jung, E., and I. Zawadzki, 2008: A study of variability of snow terminal fall velocity. *Proc. Fifth European Conf. on Radar in Meteorology and Hydrology,* Helsinki, Finland, EUMETSAT, 4 pp. [Available online at http://erad2008.fmi.fi/proceedings/extended/erad2008-0241-extended.pdf.]

Kruger, A., and W. F. Krajewski, 2002: Two-dimensional video disdrometer: A description. *J. Atmos. Oceanic Technol.,* **19,** 602–617.

Martner, B. E., R. M. Rauber, R. M. Rasmussen, E. T. Prater, and M. K. Ramamurthy, 1992: Impacts of a destructive and well-observed cross-country winter storm. *Bull. Amer. Meteor. Soc.,* **73,** 169–172.

——, J. B. Snider, R. J. Zamora, G. P. Byrd, T. A. Niziol, and P. I. Joe, 1993: A remote-sensing view of a freezing-rain storm. *Mon. Wea. Rev.,* **121,** 2562–2577.

Nešpor, V., W. F. Krajewski, and A. Kruger, 2000: Wind-induced error of raindrop size distribution measurement using a two-dimensional video disdrometer. *J. Atmos. Oceanic Technol.,* **17,** 1483–1492.

Petersen, W. A., and Coauthors, 2007: NASA GPM/PMM participation in the Canadian *CLOUDSAT*/CALIPSO Validation Project (C3VP): Physical process studies in snow. Preprints, *33rd Int. Conf. on Radar Meteorology,* Cairns, QLD, Australia, Amer. Meteor. Soc., P12A.8. [Available online at http://ams.confex.com/ams/pdfpapers/123652.pdf.]

Politovich, M. K., 1996: Response of a research aircraft to icing and evaluation of severity indices. *J. Aircr.,* **33,** 291–297.

Pruppacher, H. R., and J. D. Klett, 1997: *Microphysics of Clouds and Precipitation*. Kluwer Academic, 954 pp.

Raga, G. B., R. E. Stewart, and N. R. Donaldson, 1991: Microphysical characteristics through the melting region of a mid-latitude winter storm. *J. Atmos. Sci.,* **48,** 843–855.

Rasmussen, R., M. Dixon, S. Vasiloff, F. Hage, S. Knight, J. Vivekanandan, and M. Xu, 2003: Snow nowcasting using a real-time correlation of radar reflectivity with snow gauge accumulation. *J. Appl. Meteor.,* **42,** 20–36.

Rauber, R. M., M. K. Ramamurthy, and A. Tokay, 1994: Synoptic and mesoscale structure of a severe freezing rain event: The St. Valentine's Day ice storm. *Wea. Forecasting,* **9,** 183–208.

——, L. S. Olthoff, M. K. Ramamurthy, and K. E. Kunkel, 2000: The relative importance of warm rain and melting processes in freezing precipitation events. *J. Appl. Meteor.,* **39,** 1185–1195.

——, ——, ——, D. Miller, and K. E. Kunkel, 2001: A synoptic weather pattern and sounding-based climatology of freezing precipitation in the United States east of the Rocky Mountains. *J. Appl. Meteor.,* **40,** 1724–1747.

Roebber, P. J., S. L. Bruening, D. M. Schultz, and J. V. Cortinas Jr., 2003: Improving snowfall forecasting by diagnosing snow density. *Wea. Forecasting,* **18,** 264–287.

Ryzhkov, A. V., and D. S. Zrnić, 1998: Discrimination between rain and snow with a polarimetric radar. *J. Appl. Meteor.,* **37,** 1228–1240.

——, T. J. Schuur, D. W. Burgess, P. L. Heinselman, S. E. Giangrande, and D. S. Zrnić, 2005: The Joint Polarization Experiment: Polarimetric rainfall measurements and hydrometeor classification. *Bull. Amer. Meteor. Soc.,* **86,** 809–824.

——, G. Zhang, S. Luchs, and L. Ryzhkova, 2008: Polarimetric characteristics of snow measured by radar and 2D video disdrometer. *Proc. Fifth European Conf on Radar in Meteorology and Hydrology,* Helsinki, Finland, EUMETSAT, 4 pp. [Available online at http://erad2008.fmi.fi/proceedings/extended/erad2008-0095-extended.pdf.]

Scharfenberg, K., K. Elmore, C. Legett, and T. Schuur, 2007: Analysis of dual-pol WSR-88D base data collected during three significant winter storms. Preprints, *33rd Int. Conf. on Radar Meteorology,* Cairns, QLD, Australia, Amer. Meteor. Soc., P10.10. [Available online at http://ams.confex.com/ams/pdfpapers/123656.pdf.]

Schönhuber, M., G. Lammer, and W. L. Randeu, 2008: The 2D-video-distrometer. *Precipitation: Advances in Measurement, Estimation and Prediction,* S. C. Michaelides, Ed., Springer, 3–31.

Stewart, R. E., 1992: Precipitation types in the transition region of winter storms. *Bull. Amer. Meteor. Soc.,* **73,** 287–296.

Straka, J. M., D. S. Zrnić, and A. V. Ryzhkov, 2000: Bulk hydrometeor classification and quantification using polarimetric radar data: Synthesis of relations. *J. Appl. Meteor.,* **39,** 1341–1372.

Thurai, M., and V. N. Bringi, 2005: Drop axis ratios from a 2D video disdrometer. *J. Atmos. Oceanic Technol.,* **22,** 966–978.

——, D. Hudak, V. N. Bringi, G. W. Lee, and B. Sheppard, 2007: Cold rain event analysis using 2-D video disdrometer, C-band polarimetric radar, X-band vertically pointing Doppler radar and POSS. Preprints, *33rd Int Conf. on Radar Meteorology,*

Cairns, QLD, Australia, Amer. Meteor. Soc., 10.7A. [Available online at http://ams.confex.com/ams/pdfpapers/123251.pdf.]

Tokay, A., and Coauthors, 2007: Disdrometer derived *Z–S* relations in south central Ontario, Canada. Preprints, *33rd Int. Conf. on Radar Meteorology,* Cairns, QLD, Australia, Amer. Meteor. Soc., 8A.8. [Available online at http://ams.confex.com/ams/pdfpapers/123455.pdf.]

Trapp, R. J., D. M. Schultz, A. V. Ryzhkov, and R. L. Holle, 2001: Multiscale structure and evolution of an Oklahoma winter precipitation event. *Mon. Wea. Rev.,* **129,** 486–501.

Vivekanandan, J., S. M. Ellis, R. Oye, D. S. Zrnić, A. V. Ryzhkov, and J. Straka, 1999: Cloud microphysics retrieval using S-band dual-polarization radar measurements. *Bull. Amer. Meteor. Soc.,* **80,** 381–388.

——, G. Zhang, and M. K. Politovich, 2001: An assessment of droplet size and liquid water content derived from dual-wavelength radar measurements to the application of aircraft icing detection. *J. Atmos. Oceanic Technol.,* **18,** 1787–1798.

Yuter, S. E., D. E. Kingsmill, L. B. Nance, and M. Loffler-Mang, 2006: Observations of precipitation size and fall speed characteristics within coexisting rain and wet snow. *J. Appl. Meteor.,* **45,** 1450–1464.

Zerr, R., 1997: Freezing rain: An observational and theoretical study. *J. Appl. Meteor.,* **36,** 1647–1661.

Zhang, G., J. Vivekanandan, and E. Brandes, 2001: A method for estimating rain rate and drop size distribution form polarimetric radar measurements. *IEEE Trans. Geosci. Remote Sens.,* **39,** 831–841.

——, J. Sun, and E. A. Brandes, 2006: Improving parameterization of rain microphysics with disdrometer and radar observations. *J. Atmos. Sci.,* **63,** 1273–1290.

Zrnić, D. S., and A. V. Ryzhkov, 1999: Polarimetry for weather surveillance radars. *Bull. Amer. Meteor. Soc.,* **80,** 389–406.